0273–2289/85/1103–0029$03.20

Estimation of Intrinsic Kinetic Parameters in Tubular Enzyme Reactors by a Direct Approach

HENRIK PEDERSEN,* ENNO ADEMA,†
K. VENKATASUBRAMANIAN,‡ AND P. V. SUNDARAM§

Department of Chemical and Biochemical Engineering, Rutgers University, PO Box 909, Piscataway, NJ 08854 USA

Received February 20, 1984; Accepted May 10, 1984

ABSTRACT

A rigorous description of transport and reaction in open tubular enzyme reactors with enzymes attached to the walls of the tube—sometimes referred to as open tubular heterogeneous enzyme reactors (OTHERs)—is coupled with a general nonlinear parameter estimation routine to yield a quick and reliable method for extracting intrinsic kinetic constants from data on bulk conversion as a function of inlet concentrations and flow rates. The method is compared with previously adopted techniques based on an "apparent" rate constant concept derived from boundary layer theory and is shown to yield much more reliable estimates. The theory, presented here along with example data from the literature, is expected to be of use in the design and analysis of OTHERs in analytical and clinical applications.

Index Entries: Enzyme reactors, tubular; nonlinear parameter estimation, in tubular enzyme reactors; reactors, tubular enzyme; kinetic parameters, of tubular enzyme reactors.

*Author to whom all correspondence and reprint requests should be addressed.

†Present address: Department of Nutrition and Food Science, MIT, Cambridge, MA 02139 USA.

‡Also with: H. J. Heinz Co., World Headquarters, PO Box 57, Pittsburgh, PA 15230 USA.

§Abteilung Klinische Chemie, Poliklinik der Universitaet Goettingen, D-34, Goettingen, West Germany.

INTRODUCTION

OTHERs—Application and Description

Open tubular heterogeneous enzyme reactors, OTHERs, have been developed to exploit the unique catalytic advantages of enzymes in analytical and clinical systems. The reactors are usually prepared from small bore polymeric tubes (*1,2*), although glass tubes (*3*) and anisotropic hollow fibers (*4*) have also been used. The tubular arrangement allows for unobstructed flow paths and this feature makes them ideally suited for use in continuous-flow analyzers and as extracorporeal shunts.

In analytical applications, the OTHER has been used most extensively in continuous-flow analyzers (*5*) and is also available for commercial units. The OTHER has in addition been used in a semibatch configuration, referred to as an immobilized enzyme pipet or "impette" (*6*). When used in continuous-flow analyzers, long tubes generally lead to poor performance because of the high degree of analyte dispersion that takes place, leading to detrimental sample interference. Short tubes (with high catalytic activity) on the order of 10–20 cm length are preferred and can be used in high performance instruments at sampling rates of 150/h. In order to balance sensitivity and sampling rates, it is necessary to have available a reliable method for evaluating intrinsic enzymatic parameters in OTHERs. This information, coupled with a description of the dispersion process in the complex segmented-flow field (*7*), would allow us to approach the *a priori* design of OTHERs in continuous-flow analyzers on a sound theoretical basis.

OTHERs have also been suggested for use in clinical applications, where a "bundled" arrangement is usually preferred in order to increase the available surface area while maintaining acceptable pressure drops through the device (*8,9*). Both polymeric tubes and hollow fibers have been used; however, the hollow fiber reactor has the additional advantage of providing a separation step in series with the reaction. Thus, untoward effects associated with large molecular weight compounds circulating in the blood stream can be avoided. Information on the performance of the reactor can be used, via the concept of "bioefficacy" (*10*), to evaluate the utility of the reactor in an extracorporeal shunt.

Previous Models

Models for the design of OTHERs have been put forth by a number of workers (*11,12*) and have demonstrated how kinetic, transport, and geometrical factors affect the reactor performance. The inverse problem of evaluating the kinetic parameters from data on the reactor performance in general has received less attention, although there are numerous reports for some specific limiting situations. For instance, if the reactor surface is equiaccessible, then the usual linear plots for an enzyme-catalyzed reaction can be employed with some modifications to estimate

the intrinsic parameters for external transport limitations (*13–17*) as well as for internal or combined transport limitations (*18–23*).

For boundary layer flows in which the surface is no longer equiaccessible, some approximations are available for the inlet region of highly reactive, i.e., diffusion controlled, OTHERs (*2,24*). In these works, the average dimensionless mass transfer coefficient, Nu_m, is found from the results of Lévêque's (*25*) analysis for external flows,

$$Nu_m = 1.62\lambda^{-1/3} \tag{1}$$

where λ is the Graetz number. The overall reaction rate in an OTHER can then be easily found and is, of course, independent of the intrinsic kinetics. In a tube with no transport limitations, the integrated reaction equations are used and yield the intrinsic kinetic parameters directly.

The intermediate and general case has not been studied in great detail for OTHERs, as mentioned above, for the purpose of evaluating intrinsic parameters. In this report, we present a general computational program that allows for estimation of parameters by rigorous and efficient non-linear parameter estimation techniques. Our approach is compared with the method based on "apparent" rate constants (*24*) and is shown to yield much more reliable parameter estimates.

THEORY

Analysis of OTHERs—General Model

The general model for the OTHER is developed in this section for constant fluid properties at steady state and for a fully established laminar velocity profile. The reaction takes place at the wall in an annulus of finite thickness that may, in the case of hollow fiber reactors, be separated from the flowing reagent stream by a thin membrane or inactive region. A schematic of the cross-section is shown in Fig. 1 for two types of reactors. The governing dimensionless equations are (*11,12*):

$$L[\beta_1] = 2(1 - \rho^2)\, \partial\beta_3/\partial\lambda \tag{2}$$

$$L[\beta_3] = R(\beta_3; \boldsymbol{\kappa}) \tag{3}$$

where β_1 and β_3 are dimensionless reactant concentrations in the flow region and the reactive annulus, respectively. The dimensionless rate, R, depends on the parameters $\boldsymbol{\kappa}$. The operator L is given for cylindrical coordinates as

$$L[\bullet] = (1/\rho)(\partial/\partial\rho)[\rho\, \partial\bullet/\partial\rho] \tag{4}$$

The normalized radius, ρ, and reactor length, λ, are defined by

$$\rho = r/a \tag{5a}$$

$$\lambda = z/(aPe) \tag{5b}$$

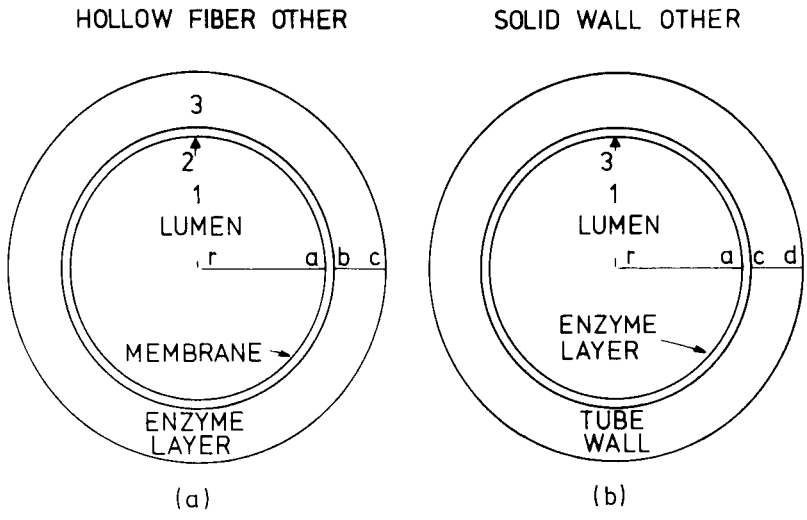

Fig. 1. Schematic illustration of the cross-section for two types of OTHERs: (a) hollow fiber and (b) solid wall (polymeric tube). The radial distances *a*, *b*, and *c* indicate the lumen (region 1), membrane (region 2), and enzyme (region 3) radii, respectively.

where a is the tube inner radius and $\mathrm{Pe} = av/D_1$ is the Peclet number based on the average velocity v and fluid diffusion coefficient D_1, corresponding to region 1. The boundary conditions are

$$\beta_1(0, \rho) = 1 \tag{6a}$$

$$\partial\beta_1/\partial\rho \,|_{\rho=0} = 0 \tag{6b}$$

$$\partial\beta_1/\partial\rho \,|_{\rho=1} = \alpha\partial\beta_3/\partial\rho \,|_{\rho=b/a} \tag{6c}$$

$$\partial\beta_1/\partial\rho \,|_{\rho=1} = -Bi_m(\beta_1 \,|_{\rho=1} - P\beta_3 \,|_{\rho=b/a}) \tag{6d}$$

$$\partial\beta_3/\partial\rho \,|_{\rho=c/a} = 0 \tag{6e}$$

The parameters α, Bi_m, and P are

$$\alpha = bD_3/aD_1 \tag{7a}$$

$$Bi_m = K_a\alpha_1/\ln(b/a) \tag{7b}$$

$$P = K_b/K_a \tag{7c}$$

The diffusion coefficient in the enzyme annulus (region 3) is D_3; K_a and K_b are the membrane/lumen and membrane/shell partition coefficients, respectively, and $\alpha_1 = D_2/D_1$ where D_2 is the membrane (region 2) diffusion coefficient.

It is assumed that the unknown parameters are embedded in the rate equation and that all other parameters are known either from separate experiments or via available correlations. The reactor experimental

data are usually available as conversions or mixing-cup concentrations as a function of inlet concentrations or flow rates. We note that varying the flow rate is analogous to changing the reactor length [cf. Eq. (5b)] provided no secondary flows are introduced. It is not uncommon, however, to measure conversions in coiled tubes that have a complex velocity profile and thus show an increased mass-transfer rate to the reactor wall region (*26*) not accounted for here. We will return to this point in the Discussion section and assume for now that the flow profile is a simple parabola, as given in the above equations. The mixing-cup concentration is found from

$$\langle\beta_1\rangle = 4\int_0^1\beta_1(1-\rho^2)\rho d\rho \tag{8}$$

and the model is reduced to the functional form,

$$\langle\beta_1\rangle = \langle\beta_1(\lambda;\ \boldsymbol{\kappa})\rangle \tag{9}$$

Limiting Models

In most applications of OTHERs, the enzyme region is a thin annulus, as shown in Fig. 1b. The boundary conditions given in Eqs. (6c)–(6e) and the diffusion equation shown in Eq. (3) can be combined and reduced to the limiting form

$$\partial\beta_1/\partial\rho\ |_{\rho=1} = -R(\beta_1|_{\rho=1}\ ;\boldsymbol{\kappa}) \tag{10}$$

This assumes that the local enzyme effectiveness factor will be approximately unity as a consequence of the thin enzyme region. In the subsequent discussion we will use this limiting form as the appropriate boundary condition.

Michaelis-Menten Kinetics

The rate expression in Eq. (9) is assumed to be of the Michaelis-Menten type for irreversible reactions

$$R(\beta;\ \kappa) = \mu\beta/(1+\omega^{-1}\beta) \tag{11}$$

where μ is the reaction modulus (a Damkoehler number)

$$\mu = ka/D_1 \tag{12}$$

and ω is the dimensionless "Michaelis constant"

$$\omega = K_m/S_0 \tag{13}$$

The enzyme rate constant is $k = V_M/K_m$ where V_M is the saturation velocity per unit area for the enzyme, and S_0 is the substrate inlet concentration. The parameters to be determined are typically k and K_m.

Linear Kinetics

In the limit $\omega^{-1} = 0$, that corresponds to small values of the inlet reactant concentration relative to the intrinsic Michaelis constant for the

immobilized enzyme, the model equations are linear. An analytical solution has been presented for this system by Kim and Cooney (*27*) that will also hold for the general three-region model, i.e., their solution depends on a single dimensionless group that is a modified modulus (*10*). It is probably advantageous, however, to solve the equations numerically since no great effort is needed when we use the methods outlined in the Appendix.

Parameter Estimation

The model $\langle\beta_1\ (\lambda;\ k,\ K_m)\rangle$ for the Michaelis-Menten kinetics gives the conversion as a function of, say, the flow rate and the inlet concentration for values of the parameters k and K_m implicitly. In order to estimate k and K_m from observed data, a nonlinear parameter estimation technique is followed (*28*).

Let the error between the model and observed values of the conversion be denoted by $\boldsymbol{\epsilon}_{ij}$ where i is a particular data point in a set of j independent variables or experiments. A weighted sum of squares S is found as

$$S(\boldsymbol{\kappa}) = \sum_{j}^{n} \boldsymbol{\epsilon}_j{}^T \mathbf{Q}_j \boldsymbol{\epsilon}_j \tag{14}$$

where $\mathbf{Q}_j$ is a symmetric weighting matrix. For maximum-likelihood estimates $\mathbf{Q}_j$ is the inverse of the covariance matrix of the experimental error. Typically, $\mathbf{Q}_j$ is approximated as a diagonal matrix. To find the minimum value of S, an iterative method is used that linearizes the model about the parameters and successively searches for smaller S. Let $\boldsymbol{\epsilon}_j{}^{(m)}$ be the mth iterate; then

$$S(\Delta\boldsymbol{\kappa}^{(m)}) = \sum_{j}^{n} (\boldsymbol{\epsilon}_j{}^{(m)} - \mathbf{D}_j\Delta\boldsymbol{\kappa}^{(m)})^T \mathbf{Q}_j\ (\boldsymbol{\epsilon}_j{}^{(m)} - \mathbf{D}_j\Delta\boldsymbol{\kappa}^{(m)}) \tag{15}$$

where $\mathbf{D}_j$ is the Jacobian found for the model evaluated at the jth experiment, with the parameter estimates of the previous iterate,

$$\mathbf{D}_j = \{\partial\chi_{ij}/\partial\kappa_p\} \tag{16}$$

The index i runs over all the data points and the p index runs over the number of parameters. Since Eq. (15) is linear in $\Delta\boldsymbol{\kappa}$, we find by setting the derivative of S with respect to $\Delta\boldsymbol{\kappa}$ equal zero,

$$\Delta\boldsymbol{\kappa}^{(m)} = \mathbf{H}^{-1} \sum_{j}^{n} \mathbf{D}_j{}^T \mathbf{Q}_j\ \boldsymbol{\epsilon}_j{}^{(m)} \tag{17}$$

and therefore an improved estimate of $\boldsymbol{\kappa}$ is found from

$$\boldsymbol{\kappa} = \boldsymbol{\kappa}^{(m)} + \Delta\boldsymbol{\kappa}^{(m)} \tag{18}$$

The matrix **H**,

$$\mathbf{H} = \sum_{j}^{n} \mathbf{D}_j^T \mathbf{Q}_j \mathbf{D}_j \tag{19}$$

is the covariance matrix of the parameter estimates and is related to the confidence intervals for the parameters. Metzler et al. (*29*) present a computer program, NONLIN, to carry out this procedure with some modifications to insure the convergence to a minimum and to handle the problem of ill-conditioned Jacobian matrices. In addition, the NONLIN program allows for constraints on the parameter space such as nonnegative values.

RESULTS AND DISCUSSION

In order to apply the parameter estimation techniques outlined above, an efficient numerical method is needed to solve the governing equations. We choose here a low-order orthogonal collocation technique in the radial direction followed by a high-order explicit ordinary differential equation solver from available computer center routines. The details are described in the Appendix. These routines when coupled with the NONLIN package provide a fast and accurate system for estimating the intrinsic kinetic parameters.

β-Galactosidase OTHER Kinetics

The data are taken from experiments with a coiled β-galactosidase OTHER (*30*). The hydrolysis of *o*-nitrophenylgalactose was followed as a function of the flow rate and the inlet concentration. The data points are plotted in Fig. 2 along with the model predictions found for the best parameter estimates of V_M and K_m where the V_M value is derived from k. For this result, we have used all five "experiments" or independent values of the flow rate simultaneously at the shown inlet concentrations. The correlation coefficient of the model to the data is given by $r^2 = 0.937$.

The model predicts higher values of the conversion at low flow rates ($Pe = 0.164$) and slightly underestimates the conversion at higher flow rates. This is most likely caused by the coiling of the tube and the induced secondary flows that take place. If we estimate k and K_m for each experiment separately, much better correlations can, of course, be obtained; however, the resulting parameter values are different for each experiment. The k value shows the largest variation from one experiment to another and will increase with increasing flow rate as one might expect

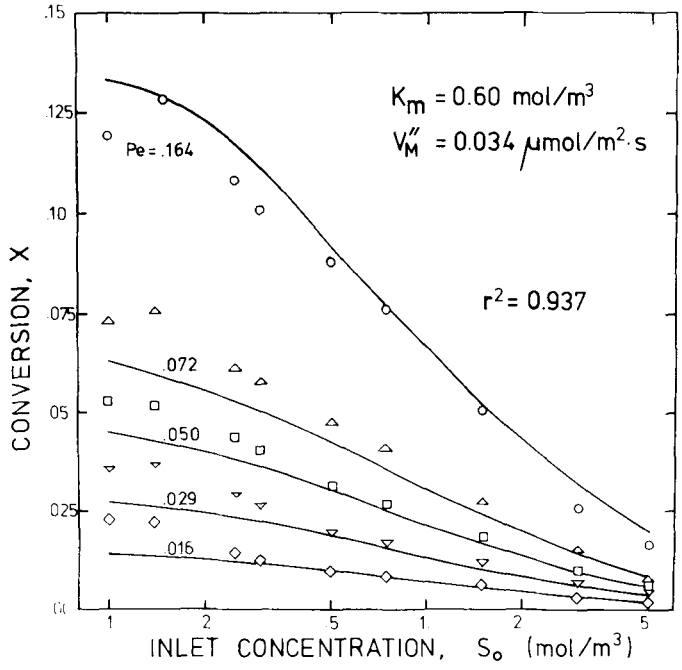

Fig. 2. Conversion as a function of the inlet concentration in a β-galactosidase OTHER for different values of Pe. The solid lines are the model predictions and the data points are from Narinesingh et al. (*30*). $D_1 = 4(10^{-5})$ cm²/s, $z = 35.8$ cm, $a = 0.05$cm. The reactant is *o*-nitrophenylgalactose.

since the secondary flows result in higher transfer rates to the wall. These interpretations should be considered with caution, however, since we are obviously not using the correct model when secondary flows are present.

An approximate 95% confidence interval for the parameters is shown in Fig. 3 along with the parameter estimates obtained for the individual experiments at the three lowest flow rates. Note that the K_m values fall within the limiting 95% confidence values, but that the k values are more widely dispersed. Nevertheless, the parameter estimates for the combined experiments are well determined. The correlation between the parameters is found from the covariance matrix of the parameter estimates and has a value of −0.86, indicating that the parameters are only slightly and negatively correlated.

The solid lines in Fig. 3 show the iterations of the NONLIN routine towards the minimum from the starting guess of $k = 1.5(10^{-7})$ m/s and $K_m = 0.3$ mol/m³. We have examined the convergence over a wide range of the parameter space and find that the same final estimate is obtained for any positive choice of parameters as an initial guess within two orders of magnitude of the final values. Therefore, the results can be surmised to represent the global minimum sum-of-squares.

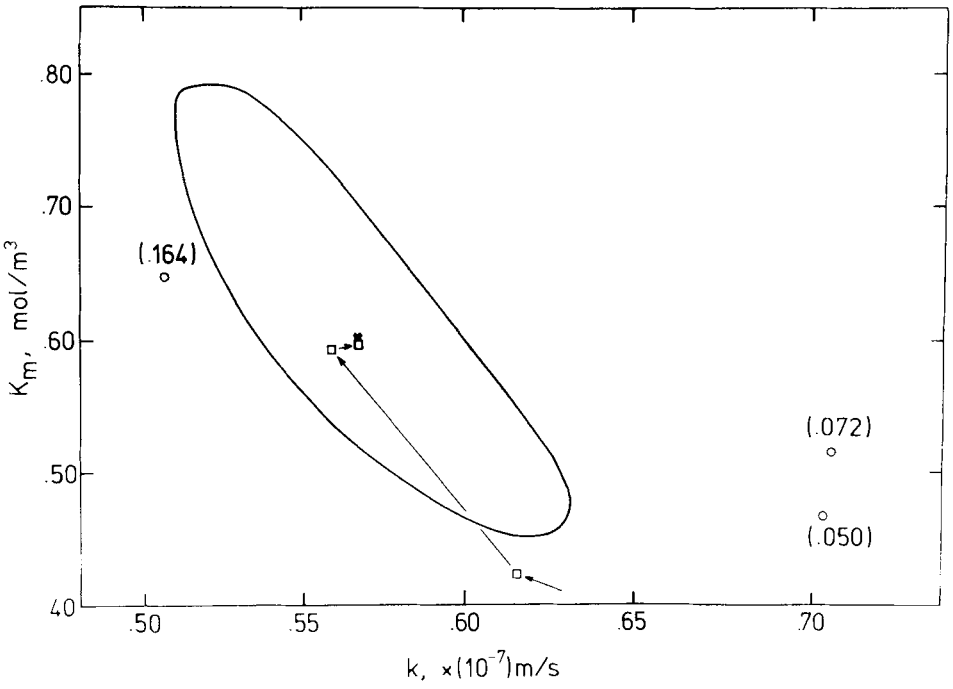

Fig. 3. Approximate joint 95% confidence contour. The best parameter estimates are located at * for all experiments combined, whereas for the individual experiments at the indicated Pe values the best parameter estimates are located at o. The iterations of the NONLIN routine to the minimum sum-of-squares is indicated by points □ starting from $K_m = 0.3$ mol/m^3 and $k = 1.5(10^{-7})$ m/s.

Comparison with the "Apparent" Rate Constant Method

Kobayashi and Laidler (*24*) have proposed an alternative method to find K_m and k values for OTHERs based on a boundary layer solution of the mass transfer equations (BL model) that has been "tested" in a series of papers (*30–32*). The theory leads to the result (our notation),

$$\omega^{app} = \omega(1 + 0.617\mu\lambda^{1/3}) \tag{20}$$

where ω^{app} is an apparent dimensionless Michaelis constant defined as the dimensionless substrate concentration for which the reaction rate is half the maximum (high S_0) reaction rate value. In order to use Eq. (20), the intrinsic rate constant V_M must first be known since it is involved in the definition of ω^{app}. Then, plotting ω^{app} against $\lambda^{1/3}$ will yield the intrinsic Michaelis constant K_m from the intercept. It is suggested in the above papers that V_M can be found from a direct plot of the data at high substrate concentrations.

The value found by Narinesingh et al. (*30*) for the data shown in Fig. 2 by this approach corresponds to $K_m = 0.18$ mol/m^3 that is, in fact, not

too different from the K_m value found for the free enzyme under identical bulk conditions. Our result, K_m = 0.60 mol/m^3, is about three times larger. The statistical accuracy of our result was checked by plotting the calculated residuals as a function of the conversion and is shown in Figs. 4 and 5 along with the residuals calculated for the BL model that lead to Eq. (20). The residuals for our approach, as shown by the thick lines in Fig. 4, are much better distributed than the values for the BL model shown by the thin lines. This is more easily seen in Fig. 5 that displays the histogram of some chosen classes of residuals. A normal (uniform) distribution about the zero value, as seen for the OTHER model, indicates an unbiased model. The BL model shows a biased representation and results derived from the BL approach should be interpreted with caution. The fact that the intrinsic K_m value increases upon immobilization of the enzyme is not caused by diffusional effects since these have been accounted for in the model, but rather reflects the change in enzymatic properties by immobilization *per se*. This may result from conformational changes, for example.

The results described above for Michaelis-Menten kinetics have also been extended to OTHERs with product inhibition and substrate inhibition (*33*). Accurate estimates of the intrinsic parameters are easily obtained provided that experimental data are available in a region where

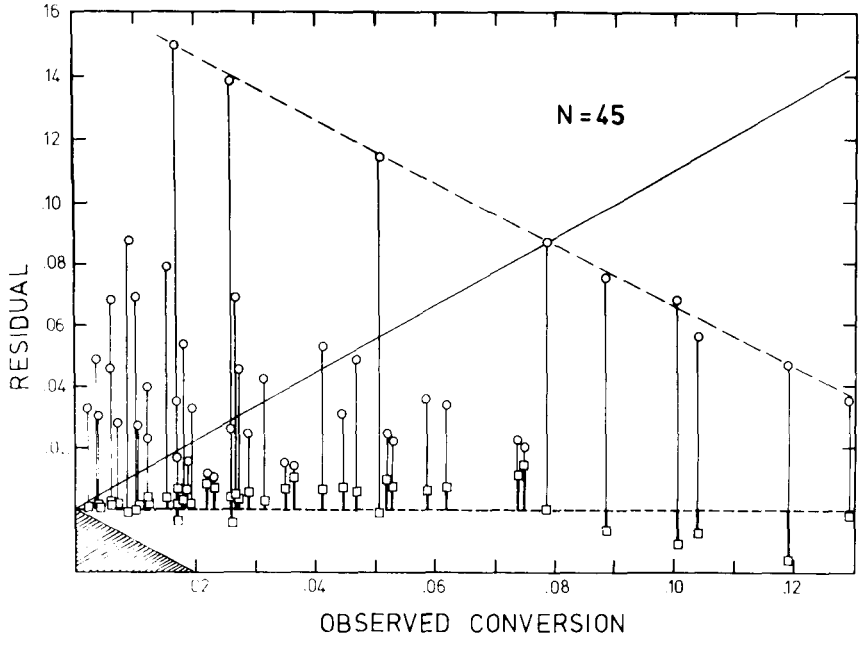

Fig. 4. Plot of the residuals (predicted − observed) versus the observed conversion for the BL model (thin lines, |) and the OTHER model (thick lines, |). The solid line indicates the residual values equal to the observed conversion. The hatched area corresponds to negative conversion values (inaccessible). The dashed line connects data points from the same experiment in the BL model and clearly indicates a trend for the residuals.

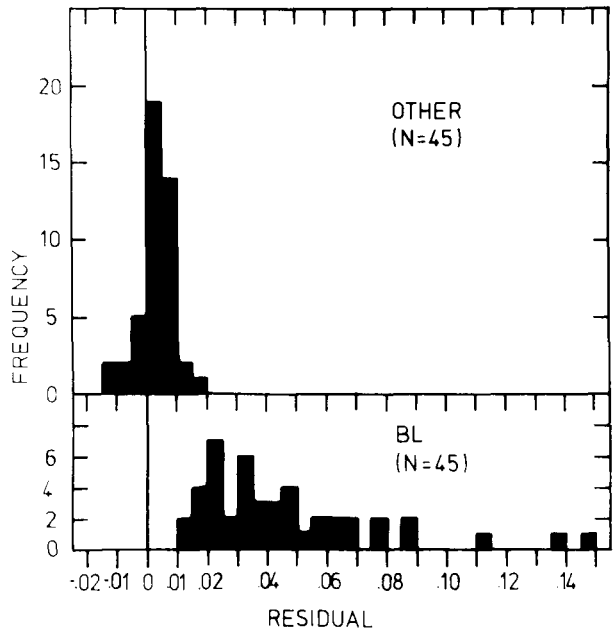

Fig. 5. Histogram of the frequency of residual observations for the OTHER model (top) and the BL model (bottom).

the complete kinetic expression can be used. That is, concentration ranges that lead to degenerate forms of the rate equation, such as in diffusion controlled OTHERs, will not allow one to obtain accurate estimates of all the parameters. The NONLIN package (*29*) will also provide selected values of the independent variables *a posteriori* that are the "best" choices for subsequent experiments in order to better estimate the parameters. These last values are found by maximizing the determinant of **H** with respect to the independent variables (*34*). In this way, the correct type of experiments to carry out are known. The sequential design of experiments and the related problem of model discrimination are discussed by Froment and Bischoff (*35*), who also provide several examples of its use in the analysis of plug-flow catalytic reactors.

CONCLUSION

The use of a boundary layer model to evaluate and extrapolate apparent rate parameters has been shown to yield unreliable estimates of the intrinsic parameters in OTHERs compared with our direct approach. This is caused by the accuracy of the starting models that are used and also to the use of Nu_m values that have been calculated under conditions of diffusion control in situations that are no longer entirely influenced by diffusion effects alone. In these situations, the Nu_m will be a function of the kinetic parameters as well (*36, 37*). For instance, if we integrate Eq. (2) to obtain the average concentration, we have

$$d\langle\beta_1\rangle/d\lambda = 2(\partial\beta_1/\partial\rho)\,|_{\rho=1} = 2R(\beta_1;\ \boldsymbol{\kappa}) \tag{21}$$

A mass transfer coefficient, Nu_m' is defined by the relation

$$\partial\beta_1/\partial\rho\,|_{\rho=1} = Nu_m'\,(\langle\beta_1\rangle - \beta_1\,|_{\rho=1}) \tag{22}$$

and one obtains an implicit equation for the surface concentation β_1.

$$R(\beta_1;\ \boldsymbol{\kappa}) = Nu_m'\,(\langle\beta_1\rangle - \beta_1) \tag{23}$$

Unfortunately, Nu_m' is not equal to Nu_m and should therefore be treated as a parameter in the problem. Such an approach has been used by Hsieh et al. (*38*) and is, in general, required when the hydrodynamics of the problem are too complex to model accurately.

Although the direct approach may seem cumbersome to handle, it is easily implemented on a computer. Unlike the BL model, various rate laws can be tested that may aid in the discrimination between competing models. In this way, experimental design, parameter estimation, and model discrimination can be reduced to routine practice for the analysis of reactors with immobilized enzymes.

NOMENCLATURE

a	Tube inner diameter, m
A_{ij}	Collocation matrix for first derivatives
b, c, d	Tube radii shown in Fig. 1, m
B_{ij}	Collocation matrix for second derivatives
Bi_m	Biot number, $= K_a\alpha_1/\ln(b/a)$
D_1, D_2, D_3	Diffusion coefficients in regions 1, 2, 3 (m^2/s)
$\mathbf{D}_j$	Jacobian matrix
$\mathbf{H}$	Matrix defined in Eq. (19)
k	Enzyme rate constant $= V_M/K_m$, m/s
k_L	Mass transfer coefficient, m/s
K_m	Intrinsic Michaelis constant, mol/m^3
K_a, K_b	Partition coefficients
$\mathbf{M}$	Matrix defined in Eq. (A9)
Nu_m	Mass transfer coefficient, $2ak_L/D_1$
P	Ratio of partition coefficients
Pe	Peclet number, av/D_1
$\mathbf{Q}_j$	Weighting matrix
r	Tube radial coordinate, m
R	Dimensionless rate
S	Sum of squares
S_0	Inlet reactant concentration, mol/m^3
v	Average fluid velocity, m/s
$\mathbf{w}$	Vector of integration (Radau) weights
V_M	Maximum reaction rate, mol/m^2s
z	Tube length coordinate, m

Greek symbols

α, α_1	bD_3/aD_1, $= D_2/D_1$
β_1, β_3	Dimensionless reactant concentration in regions 1, 3
$\boldsymbol{\beta}_1$	Vector of dimensionless concentrations
$\boldsymbol{\epsilon}$	Error vector
$\boldsymbol{\kappa}$, $\Delta\boldsymbol{\kappa}$	Parameter vector, correction vector
λ	Dimensionless length, z/aPe
μ	Modulus, ka/D_1
ρ	Dimensionless radius, r/a
ω	Dimensionless Michaelis constant, K_m/S_0

Superscripts

app	Apparent value
m	mth iteration
T	Transpose
$'$	Influenced by kinetics
$\tilde{}$	Approximation

Subscripts

i, j, p	Counting indices
1, 2, 3	Region indices

REFERENCES

1. Sundaram, P. V., and Hornby, W. E. (1970), *FEBS Lett.* **10,** 325.
2. Horváth, Cs., Solomon, B. A. (1972), *Biotechnol. Bioeng.* **14,** 885.
3. Itoh, N., Hagi, N., Iida, T., Tanaka, A., and Fukui, S. (1979), *J. Appl. Biochem.* **1,** 291.
4. Pedersen, H., Horváth, Cs., and Ambrus, C. (1978), *Res. Commun. Chem. Pathol. Pharmacol.* **20,** 559.
5. Pedersen, H., and Horváth, Cs. (1981), in *Applied Biochemistry and Bioengineering*, **3,** Wingard, L. B., Katchalski-Katzir, E., and Goldstein, L., eds., Academic Press, New York, pp. 1–96.
6. Sundaram, P. V., and Jayaraman, S. (1979), *Clin. Chim. Acta* **94,** 309.
7. Pedersen, H., and Horváth, Cs. (1981), *Ind. Eng. Chem. Fundam.* **20,** 411.
8. Ambrus, C., Ambrus, J., Horváth, Cs., Pedersen, H., Sharma, S., Kant, C., Mirand, E., Guthrie, R., and Paul, T. (1978), *Science* **201,** 837.
9. Kanales, J. J., and Kitto, G. B. (1981), *J. Appl. Biochem.* **3,** 387.
10. Pedersen, H., and Horváth, Cs. (1982), *J. Pharmacokin. Biopharm.* **10,** 437.
11. Horváth, Cs., Shendalman, L. H., and Light, R. T. (1973), *Chem. Eng. Sci.* **28,** 375.
12. Waterland, L. R., Michaels, A. S., and Robertson, C. R. (1974), *AIChE J.* **20,** 50.
13. Hornby, W. E., Lilly, M. D., and Crook, E. M. (1968), *Biochem. J.* **107,** 669.
14. Shuler, M. L., Aris, R., and Tsuchiya, H. M. (1972), *J. Theor. Biol.* **35,** 67.
15. Kobayashi, T., and Laidler, K. J. (1974), *Biotechnol. Bioeng.* **16,** 77.
16. Horváth, Cs., and Engasser, J.-M. (1974), *Biotechnol. Bioeng.* **16,** 909.

17. Engasser, J.-M., Coulet, P., and Gautheron, D. C. (1977), *J. Biol. Chem.* **252,** 7919.
18. Moo-Young, M., and Kobayashi, T. (1972), *Can. J. Chem. Eng.* **50,** 162.
19. Engasser, J.-M., and Horváth, Cs. (1973), *J. Theor. Biol.* **42,** 137.
20. Regan, D. L., Lilly, M. D., and Dunnill, P. (1974), *Biotechnol. Bioeng.* **16,** 1081.
21. Hamilton, B., Gardner, C. R., and Colton, C. K. (1974), *AIChE J.* **20,** 503.
22. Gondo, S., Isayama, S., and Kasunobi, K. (1975), *Biotechnol. Bioeng.* **17,** 423.
23. Lee, G. K., Lesch, R. A., and Reilly, P. J. (1981), *Biotechnol. Bioeng.* **23,** 487.
24. Kobayashi, T., and Laidler, K. J. (1974), *Biotechnol. Bioeng.* **16,** 99.
25. Lévêque, M. A. (1928), *Annals Mines* **13,** 201.
26. Carbonell, R. G. (1975), *Biotechnol. Bioeng.* **17,** 1383.
27. Kim, S. S., and Cooney, D. O. (1976), *Chem. Eng. Sci.* **31,** 289.
28. Seinfeld, J., and Lapidus, L. (1970), *Process Modeling, Estimation and Identification,* Prentice-Hall, Englewood Cliffs, NJ, pp. 383–401.
29. Metzler, C. M., Elfring, G. L., and McEwen, A. J. (1974), *Biometrics* **30,** 562.
30. Narinesingh, D., Ngo, T. T., and Laidler, K. J. (1975), *Can. J. Biochem.* **53,** 1061.
31. Bunting, P. S., and Laidler, K. J. (1974), *Biotechnol. Bioeng.* **16,** 119.
32. Ngo, T. T., Narinesingh, D., and Laidler, K. J. (1976), *Biotechnol. Bioeng.* **18,** 119.
33. Adema, E. (1983), M. S. Thesis, Department of Chemical and Biochemical Engineering, Rutgers University, New Brunswick, NJ.
34. Box, G. E. P. and Lucas, H. L. (1959), *Biometrika* **46,** 77.
35. Froment, G., and Bischoff, K. (1979), *Chemical Reactor Analysis and Design,* John Wiley, New York, NY, pp. 106–132.
36. Rosner, D. E. (1964), *AIAA J.* **2,** 593.
37. Sucker, D., and Brauer, H. (1979), *Warme- und Stoffubertragung* **12,** 35.
38. Hsieh, F., Davidson, B., and Vieth, W. R. (1976), *J. Appl. Chem. Biotechnol.* **26,** 631.
39. Baden, N., and Villadsen, J. V. (1982), *Chem. Eng. J.* **23,** 1.
40. Villadsen, J. V., and Stewart, W. E. (1967), *Chem. Eng. Sci.* **22,** 1483.
41. Finlayson, B. A. (1972), *The Method of Weighted Residuals and Variational Principles,* Academic Press, New York, NY.
42. Villadsen, J. V., and Michelsen, M. L. (1978), *Solution of Differential Equation Models by Polynomial Approximation,* Prentice-Hall, Englewood Cliffs, NJ.
43. IMSL (1982), International Mathematical and Statistical Libraries, Inc., Vers. 9, Houston, TX.

APPENDIX

Baden and Villadsen (*39*) have shown how collocation methods can be effectively used in parameter estimation routines for differential equation models. Our approach is a modification of their method since we have found it expeditious to combine collocation techniques in the radial direction with an explicit Runge-Kutta technique in the axial direction rather than making use of a complete "double" collocation solution.

An approximate polynomial solution is assumed for β_1 that is designated as $\tilde{\boldsymbol{\beta}}_1$ and takes the form (*40*)

$$\tilde{\boldsymbol{\beta}}_1 = \sum_{i=0}^{N} a_i(\lambda)\rho^{2i} \qquad 0 \leq \rho \leq 1 \tag{A1}$$

This form automatically satisfies the boundary condition at $\rho = 0$ so that one need only be concerned with the boundary condition at $\rho = 1$. An equivalent expression is (*41,42*),

$$\tilde{\boldsymbol{\beta}}_1 = \sum_{i=1}^{N+1} \Xi_i(\rho)\tilde{\boldsymbol{\beta}}_1(\lambda, \rho_i) \tag{A2}$$

where Ξ_i is the Lagrange interpolation polynomial

$$\Xi_i(\rho) = \prod_{\substack{i \neq j \\ j=1}}^{N+1} (\rho^2 - \rho_j^2) \Big/ \prod_{\substack{i \neq j \\ j=1}}^{N+1} (\rho_i^2 - \rho_j^2) \tag{A3}$$

From Eq. (A2), the derivatives are easily calculated as

$$\left.\frac{d\tilde{\boldsymbol{\beta}}_1}{d\rho}\right|_{\rho_i} = \sum_{i=1}^{N+1} \left.\frac{d\Xi_i}{d\rho}\right|_{\rho_i} \tilde{\boldsymbol{\beta}}_1(\lambda, \rho_i) = \sum_{i=1}^{N+1} A_{ji}\tilde{\boldsymbol{\beta}}_{1i} \tag{A4}$$

$$\left.\frac{d^2\tilde{\boldsymbol{\beta}}_1}{d\rho^2}\right|_{\rho_i} = \sum_{i=1}^{N+1} \left.\frac{d^2\Xi_i}{d\rho^2}\right|_{\rho_i} \boldsymbol{\beta}_1(\lambda, \rho_i) = \sum_{i=1}^{N+1} B_{ji}\boldsymbol{\beta}_{1i} \qquad {}_{i=1}^{N+1} \tag{A5}$$

Eliminating the wall concentration through the (nonlinear) Eq. (5f) and Eq. (A4) yields an initial value problem

$$d\tilde{\boldsymbol{\beta}}_1/d\lambda = \mathbf{L}[\tilde{\boldsymbol{\beta}}_1] \tag{A6}$$

$$\tilde{\boldsymbol{\beta}}_1(0) = 1 \tag{A7}$$

The operator $\mathbf{L}$ is now

$$\mathbf{L}[\tilde{\boldsymbol{\beta}}_1] = \mathbf{M}\tilde{\boldsymbol{\beta}}_1 + \mathbf{f}(\tilde{\boldsymbol{\beta}}_1; \boldsymbol{\kappa}) \tag{A8}$$

where $\tilde{\boldsymbol{\beta}}_1$ is the vector of concentration values and

$$M_{ij} = 4(\rho_i^2 B_{ij} + A_{ij})/(1 - \rho_i^2) \quad i, j = 1,2, \ldots N \tag{A9}$$

$$f_i = M_{iN+1}\,[-b + \sqrt{(b^2 - 4ac)}]/2a \tag{A10}$$

$$a = \omega^{-1} A_{N+1,\,N+1} \tag{A11}$$

$$b = c\omega^{-1} + \mu + A_{N+1,\,N+1} \tag{A12}$$

$$c = \sum_{j=1}^{N} A_{N+1j}\tilde{\boldsymbol{\beta}}_{1j} \tag{A13}$$

The roots ρ_i^2 are found as the zeros of the $P_N^{(2,\ 0)}(\rho^2)$ Jacobi polynomial (*42*). The average concentration is calculated as

$$\langle\tilde{\boldsymbol{\beta}}_1\rangle = \mathbf{w}^T\tilde{\boldsymbol{\beta}}_1 \tag{A14}$$

where **w** is the vector of Radau weights (*42*).

We chose $N = 4$ in our approximation as being sufficiently accurate for all model results and solve the initial value problem by a 5th–6th order Runge-Kutta method, DVERK, from the IMSL (*43*) library. Approximate computation times are about 3–5 s on an AS/9000-2 computer for the entire parameter estimation routine with all data points included. A listing of the computer program is available from the authors.